Directional Element Evaluation Applied to Half-wavelength Transmission Lines

Juan D. Villón Berrocal, Maria C. Tavares

***Abstract*—In this paper, a careful analysis of directional element behavior applied to a half-wavelength transmission line (HWL) is presented. Single line-to-ground (SLG) faults were applied, varying loading conditions and fault resistance. A commercial relay was used. Two directional elements were considered: 32QG and 32V. With the aim of obtaining directional element setting parameters, a Python program based on two-port network theory was developed. The simulations were also performed in a hardware-in-the-loop (HIL) environment. It was observed that only the element 32V operated properly throughout the system during SLG fault conditions. It can be concluded that the conventional directional element algorithm can be applied to a system with a half-wavelength transmission line under the above-mentioned fault condition.**

***Keywords*—Directional function, half-wavelength transmission, HIL, real-time simulation.**

I. Introduction

In Brazil, due to the increasing demand for electric power in recent years, it is necessary to enlarge energy sources. The country has a large hydroelectric potential not yet explored in its northern region. However, this region is located far away from the southeast and northeast regions, which have the largest energy consumption [1]. Consequently, there is a need to connect these regions to transport huge energy blocks over very long distances. This problem also occurs in other countries with similar continental dimensions, such as China and Russia.

HVDC technology is currently the widely adopted power transmission solution for very long distance. However, the half-wavelength power transmission line (HWL) is a robust AC alternative to this technology. This very long non-conventional line (length of 2500 km for a 60 Hz power system) does not demand intermediate substations, being a point-to-point AC transmission system. Moreover, it presents unitary Ferranti Effect, which eliminates the need of reactive power support for different loading operation conditions [2]. Research conducted by [3] shows a saving of 25% when compared to HVDC line cost with similar power capacity. On the other hand, it is possible to obtain transmission lines shorter than 2500 km with similar behavior to HWL line, using tuning equipment [4], [5].

An important topic that still needs a major contribution is protection. There are currently studies about fault detection, fault location, fault phase selector and overvoltage control for critical faults. However, an important protection function, also known as the directional element, has not been evaluated. This element allows operation when the fault is in the forward direction and should prevent any operation for reverse faults. Therefore, it is necessary to verify the performance of the directional element for the HWL lines.

The present paper outlines the performance of a conventional directional element applied to an HWL line. The test system is composed of an 800 kV 2600-km long line. A real time hardware-in-the-loop (HIL) test system was implemented using the RTDS simulator for testing a commercial distance protection relay, SEL-421. It was noted that only one directional element (32V) protected the whole system during single line-to-ground fault (SLG) conditions. Additionally, a procedure to set the directional element for the HWL is proposed.

II. Half-Wavelength Transmission Line

HWL and conventional lines present different electrical behavior. In this section, we summarize HWL characteristics and some recent studies about this non-conventional line.

A. Fundamental Characteristics

Formerly, the steady-state response of HWL line will be considered. Equation (1) describes the relationship between the voltage and current of the line sending terminal (V_s and I_s) with the voltage and current at a distance x from it (V_x and I_x) [6]. The line propagation constant (γ) derives from the positive sequence impedance (Z_L) and admittance (Y_L) per unit length.

$$\begin{bmatrix} V_x \\ I_x \end{bmatrix} = \begin{bmatrix} \cosh(\gamma x) & -Z_C \sinh(\gamma x) \\ -\frac{1}{Z_C}\sinh(\gamma x) & \cosh(\gamma x) \end{bmatrix} \begin{bmatrix} V_s \\ I_s \end{bmatrix} \quad (1)$$

If $x = L$, where L is the line length, the voltage and current at the receiving terminal can be determined ($V_x = V_R$ and $I_x = I_R$). For the HWL line under study ($L = 2600\ km$, $\gamma = 2.61 \times 10^{-5} + j\ 128.77 \times 10^{-5} [km^{-1}]$, $Z_C = 131.45 - j\ 2.66\ \Omega$), and no load condition ($I_R = 0$):

$$\left| \frac{V_R}{V_S} \right| = 1.02 \quad (2)$$

It can be seen in (2) that the voltage magnitudes at line terminals will have almost equal value in an ideal half-wavelength transmission line. Therefore, this type of line has unitary Ferranti Effect, that is to say, it does not need compensation to maintain the voltage at the remote terminal

This study was supported by the research agencies CAPES (code 001), CNPq and FAPESP (2017/20010-1). The authors are with the School of Electrical and Computer Engineering, University of Campinas, Brazil (e-mail: jvillonb@dsce.fee.unicamp.br; ctavares@unicamp.br).

Paper submitted to the International Conference on Power Systems Transients (IPST2021) in Belo Horizonte, Brazil June 6-10, 2021.

similar to the nominal value in light or no loading operation condition.

A line with a little longer than the half-wavelength transmission line (2600 km) shows good performance with respect to stability [7]. Hereinafter, this transmission will be termed a little more half-wavelength transmission lines or HWL+ in short.

B. Study of the Protection System of HWL+ Line

In the last years several researchers have been studying HWL protection. Below we summarize some of them.

In [8], a commercial distance relay manage to protect the whole HWL for SLG faults. The function 59N, based on instantaneous zero sequence voltage, was necessary to identify faults in the whole line. Similar research shows the results on HWL+ protection scheme for three-phase faults [9]. It was possible to protect this line with two conventional relays.

A two-terminal impedance-based fault location algorithm for HWL was proposed by [10], with high reliability. Another fault location was suggested by [11], based on the traveling wave theory. The method presented a very good performance, with small error.

Finally, in [12], an innovative faulted-phase selector element is proposed for HWL lines. HIL tests were implemented with RTDS and the new algorithm was coded in SEL-421 programmable area. The new element successfully operated for all types of faults along the entire HWL line.

III. Directional Element

Directional element is an essential protection function that offers security and selectivity. This element determines fault direction (forward or reverse) with reference to relay. With this declaration of fault direction, protection will identify if the fault occurs inside or outside the area to be protected [13].

A. Directional Element Classic Concepts

Torque concept was used by the classic directional element for several years [14]. However, in specific cases, the torque measurement was too small, which could generate incorrect declaration of fault direction [13]. Thus, a new directional element used in several commercial relays was developed, based on the negative sequence impedance. Fig. 1 [13] shows a system in sequence components with SLG fault condition (R_F: fault resistance). The system has two sources (ES and ER), which are connected by a transmission line with impedance Z_L. In the negative sequence circuit, the relay measures $-I_{R2}$ for reverse faults and I_{R2} for forwarding faults, so negative sequence impedances (Z_2), for both cases, are calculated in (3) and (4).

$$Z_{2(ForwardFaults)} = V_2/I_{S2} = -Z_{S2} \tag{3}$$

$$Z_{2(ReverseFaults)} = V_2/(-I_{S2}) = Z_{L2} + Z_{R2} \tag{4}$$

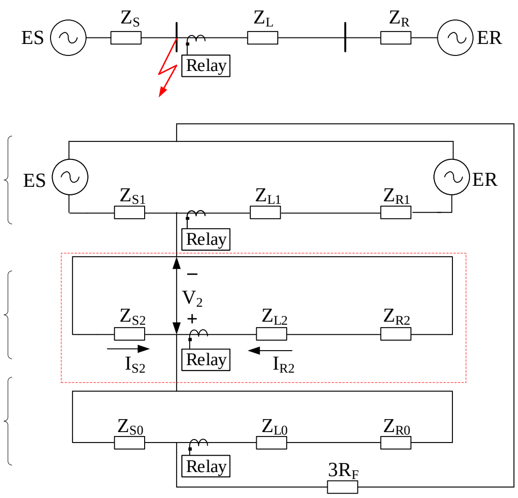

Fig. 1. Sequence components diagram for single-line-to-ground faults

B. SEL-421 Directional Elements

The SEL-421 distance relay was used for the test. This equipment offers three directional elements for ground faults: 32QG (negative-sequence voltage polarized for faults involving ground), 32V (zero-sequence voltage polarized) and 32I (zero-sequence current polarized). Also, it has one directional element for line-to-line faults: 32Q (negative-sequence voltage polarized for phase faults) [15].

The elements 32QG and 32Q calculate the impedance z2 (5) to obtain fault direction. This impedance depends on negative-sequence voltage and current, and positive-sequence impedance of the protected line [13]. In a similar way to obtain fault direction, the 32V element calculates the impedance z0 (6), which depends on zero-sequence voltage, current, and impedance of the protected line. Moreover, the 32I element does not use any impedance to find the fault direction. This element calculates the direction using the zero sequence current (I_0) and the polarization current (I_P) (7).

$$z2 = Re[V_2.(1\angle Z1ANG.I_2)^*]/|I_2|^2 \tag{5}$$

$$z0 = Re[3V_0.(1\angle Z0ANG.I_G)^*]/|I_G|^2 \tag{6}$$

$$32I = Re[(3I_0.I_P^*)] \tag{7}$$

Each directional element described uses two directional bits that represent the fault direction. Directional bits depend on setting parameters, which are described below.

- 50FP: Threshold current that enables forward fault decisions. In the case of 32QG element, if the $3I_2$ magnitude (I_2 is the negative sequence current measured in the relay) is greater than 50FP, the directional element will process the fault direction. For the 32V and 32I elements, this parameter is compared to the I_G current ($I_G = 3I_0$).

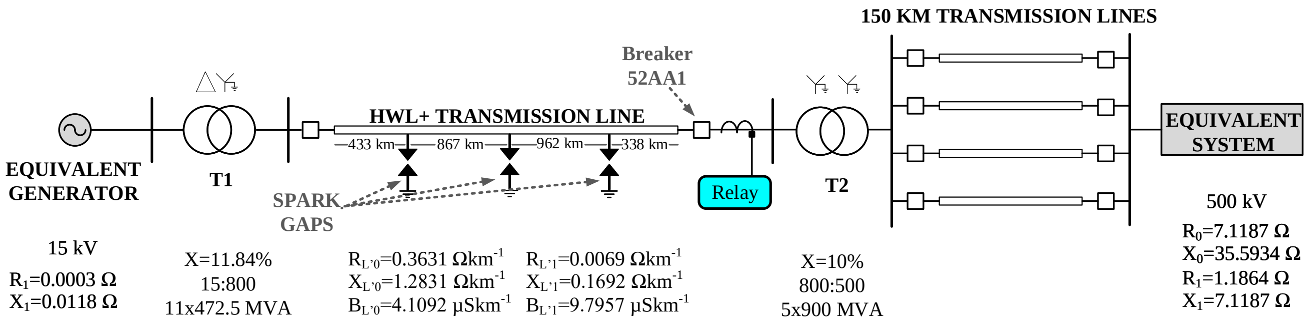

Fig. 2. Test System including 800 kV HWL+

- 50RP: Threshold current that enables reverse fault decisions. This parameter acts similarly to 50FP parameter.
- Z2F: Negative sequence impedance threshold for forward faults.
- Z2R: Negative sequence impedance threshold for reverse faults.
- a2: Positive sequence restraint factor, which restricts the relationship between the negative and positive sequence current I_2/I_1 measured in the relay.
- k2: Zero sequence restraint factor. Similarly to a2, k2 restricts the relationship between the negative and zero sequence current I_2/I_0 measured in the relay.
- Z0F: Zero sequence impedance threshold for forward faults.
- Z0R: Zero sequence impedance threshold for reverse faults.
- a0: Positive sequence restraint factor. It restricts the relationship between the zero and positive sequence current I_0/I_1 measured in the relay.

Table I shows the setting parameters used for each directional element.

TABLE I
SEL-421 Directional Elements

Directional Element	Directional Bits		Setting parameters
	Forward Faults	Reverse Faults	
32QG	F32QG	R32QG	50FP, 50RP, Z2F, Z2R, a2, k2.
32V	F32V	R32V	50FP, 50RP, Z0F, Z0R, a0.
32I	F32I	R32I	50FP, 50RP, a0.

IV. Use of Two-port Networks to Obtain Directional Element Settings Parameters

Two-port networks element theory are commonly used to obtain a steady-state response for fundamental frequency, but they can be applied to calculate phasors under unbalanced conditions. This element is sometimes called coupling network, or four poles, or two terminal pair (just to name a few), and might contain a transmission line model or a fault model [16]. It should be noted that this method is much less time-consuming to obtain phasor data than simulations performed by time-domain, such as PSCAD or ATP, which include transient response in their simulation.

In the regular application for fundamental frequency analysis under balanced condition, the power system is modeled as a single-phase circuit (positive sequence) and the two-port element will have two-port at each terminal. For unbalanced analysis, the power system is represented as a three-phase system, and the two-port element will have 6 ports at each terminal. For instance, in (8), the matrix of order 6 represents a three-phase transmission line model, which contains four sub-matrices (A^{abc}, B^{abc}, C^{abc}, D^{abc}), of order 3, a classical approach also described by [17]. Also, there are phase voltages (V_{Sa}, V_{Sb}, V_{Sc}, V_{Ra}, V_{Rb} and V_{Rc}) and line currents (I_{Sa}, I_{Sb}, I_{Sc}, I_{Ra}, I_{Rb} and I_{Rc}) in each terminal (S and R), assuming the current flows from S to R.

$$\begin{bmatrix} V_{Sa} \\ V_{Sb} \\ V_{Sc} \\ I_{Sa} \\ I_{Sb} \\ I_{Sc} \end{bmatrix} = \begin{bmatrix} A^{abc} & B^{abc} \\ C^{abc} & D^{abc} \end{bmatrix} \times \begin{bmatrix} V_{Ra} \\ V_{Rb} \\ V_{Rc} \\ I_{Ra} \\ I_{Rb} \\ I_{Rc} \end{bmatrix} \tag{8}$$

V. Test System

The system tested has an 800 kV HWL+ transmission line with 2600 km, which connects a generator to an equivalent system, in the source-grid system presented in Fig. 2. The HWL+ line presents a surge impedance loading (SIL) of 4867 MW and the bundle geometry is optimized as described by [18]. The HWL must transport only active power, the same way as a HVDC Link. An adequate operational condition would consider unitary power factor (pf) for heavy loads and a small deviation, from 0.925 to 0.95 for light loading [5]. For this study we have adopted pf = 1.

Spark-gaps (SG) were placed in three specific points (one spark-gap per phase). The location and operation of these devices are described by [19]. They are necessary to detune resonant condition for non-zero (balanced) sequence faults. They will not operate for SLG faults, but will act for the remainder faults. As two-port elements are used for phasor analysis, no SG operation was modeled in this stage of the study, only in HIL study.

The equivalent generation system is composed of 11 generators of 15 kV totaling 5197.5 MW. In this case, the parameters of the Serra da Mesa (Brazil) power plant generators [20] were used. The generation system was connected to the HWL+ line through a transformer which is equivalent to actual 11 step-up transformers (T1).

To connect the equivalent system to the HWL+ line receiving terminal another transformer (T2) followed by four parallel conventional 500 kV lines was used. The transformer T2 is equivalent to 5 step-down transformers, which has a total power of 4500 MVA. Each conventional line presents a SIL of 1175 MW, and the data are described by [21].

VI. Results

The directional element operation results are shown in this section. The relay was positioned at the receiving terminal (Fig. 2). The HWL operating conditions are shown in Table II and were calculated for two loading levels with a unitary power factor at receiving terminal.

TABLE II
Equivalent Sources Voltages Data

SIL level	$\hat{V}_G[kV]$ (Equivalent Generator Voltage)	$\hat{V}_E[kV]$ (Equivalent System Voltage)
0.1 SIL	$13.77\angle -204.1°$	$468.79\angle -1.73°$
1.0 SIL	$17.22\angle -178.44°$	$489.47\angle -25°$

The system was simulated for SLG faults. These faults were applied along the HWL+ line and one of the four 150 km transmission lines, also varying fault resistance (1 Ω and 10 Ω). In order to obtain adequate setting parameters, previously the system was modeled under fault condition using the two-port network theory. Then, the SEL-421 relay directional element configuration was adjusted with these parameters. Eventually, the system was simulated again using the RTDS together with the relay and an amplifier (Doble F6350) in a real time digital hardware-in-the-loop (HIL) test (Fig. 3).

A Python program was used to model the system (under SLG faults) with two-port networks (Appendix). Then, voltages and currents (I_1, I_2, I_0, V_1, V_2, and V_0) were obtained at the receiving terminal. These measurements were used to obtain values related to directional element parameter settings ($3I_2$, I_2/I_1, I_2/I_0,I_G, and I_0/I_1). Later on, these values were further adjusted to obtain feasible parameters. An example is explained in the next subsection.

The voltages at the receiving terminal were obtained at the secondary side of the potential transformers (PT), with a transformation ratio of 800:0.11. The currents were obtained at the secondary side of the current transformers (CT), with a transformation ratio of 1500:5. Both instrument transformers were considered ideal.

The response of the directional element for each fault was monitored in the RTDS. The HWL+ was modeled both with

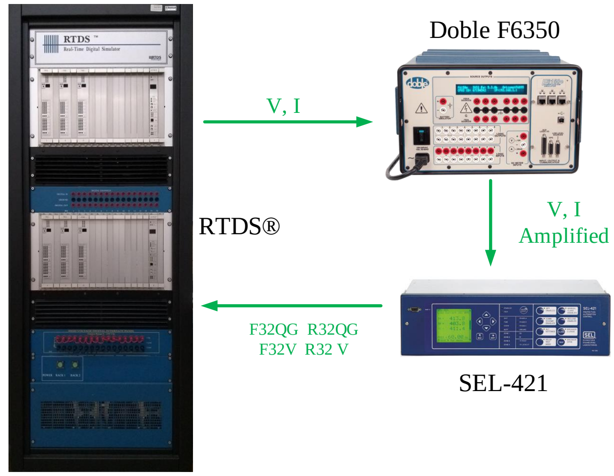

Fig. 3. HIL setup

distributed parameters and frequency dependent (phase) model in RTDS simulations. For the present analysis the results were similar.

A flow chart of the test sequence is given in Fig. 4.

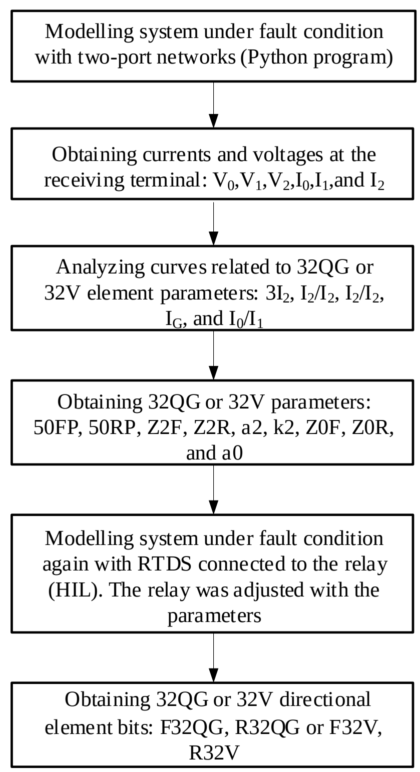

Fig. 4. Flow chart of the test sequence

A. Parameter Settings of the Directional Elements

Because the transformer close to relay is wye-grounded wye-grounded, the 32I element was not used in this research.

This element depends on polarization current (Ip), and it is not effective for this type of transformer. For instance, if a fault is applied in the high voltage side, the polarization current will flow up the neutral on the high side and down the neutral on the low side. The contrary occurs for faults in the down voltage side. Hence a relay connected to a CT located in either of the neutrals will not determine correctly the fault direction [22], [23].

In the relay global parameters section, it is necessary to input the sequence series impedances of transmission line where the relay is located. Thus, the sequence impedances of the HWL+ line were obtained by calculating the apparent impedance seen by the sending terminal S ($Z_S = V_S/I_S$), when the receiving terminal is short-circuited ($V_R = 0$). Dividing these impedances by the PT and CT transformation ratios, we have: $Z_{1(HWL+)} = Z_{2(HWL+)} = 1.19\angle 70.12°\Omega$ and $Z_{0(HWL+)} = 16.93\angle -18.65°\Omega$.

Note that the angle of $Z_{0(HWL+)}$ has a negative value ($-18.65°$). This parameter cannot be inputted to the relay global configuration, which only accepts positive values. Therefore, the minimum value ($5°$) was set for both directional elements. The operation of the 32QG element will not be compromised, since this angle is not used in the direction calculation. The contrary occurs with the 32V element, which calculates z0 (6). The value will not be the correct one, but it will be the one necessary to have steady element performance.

The directional element parameters were chosen by analyzing curves that depend on the sequence current and the impedance measured by the relay for the different fault conditions previously described.

The 32QG element has 6 setting parameters shown in Table I. The parameters 50FP and 50RP depend on $3I_2$, so it is necessary to obtain this value for different fault locations. The curves $3I_2$ of all simulated cases, applying AG faults are shown in Fig. 5. It can be seen that the lowest value for all the cases (0.336 A) is located at a distance of 440 km ahead of the relay. For a correct relay operation, the minimum value was inserted for these parameters (50FP = 50RP = 0.25).

For the parameters a2 (I_2/I_1) and k2 (I_2/I_0), similar analyses were conducted. The lowest I_2/I_1 value for all four cases is 0.012. It is not possible to use this value since it is below the a2 minimum limit (0.02). Therefore, the minimum value was set (a2 = 0.02). Because k2 has the same restriction ($I_2/I_{0\ \mathrm{min}}$ = 0.058), the lower limit was set (k2 = 0.1).

Using the Equation (5), we have z2 = -2.405 Ω for forward faults and z2 = 3.343 Ω for reverse faults. Then, Z2F = 0 Ω and Z2R = 0.1 Ω were chosen for proper operation.

It is expected that 32QG element will not correctly work in parts of HWL+ because of the cited adjusts.

Similar analyses were conducted for the 32V element. Moreover, it was possible to set correct parameters in contrast with the above-mentioned element.

The 32QG and 32V element parameters for SLG faults are shown in Table III.

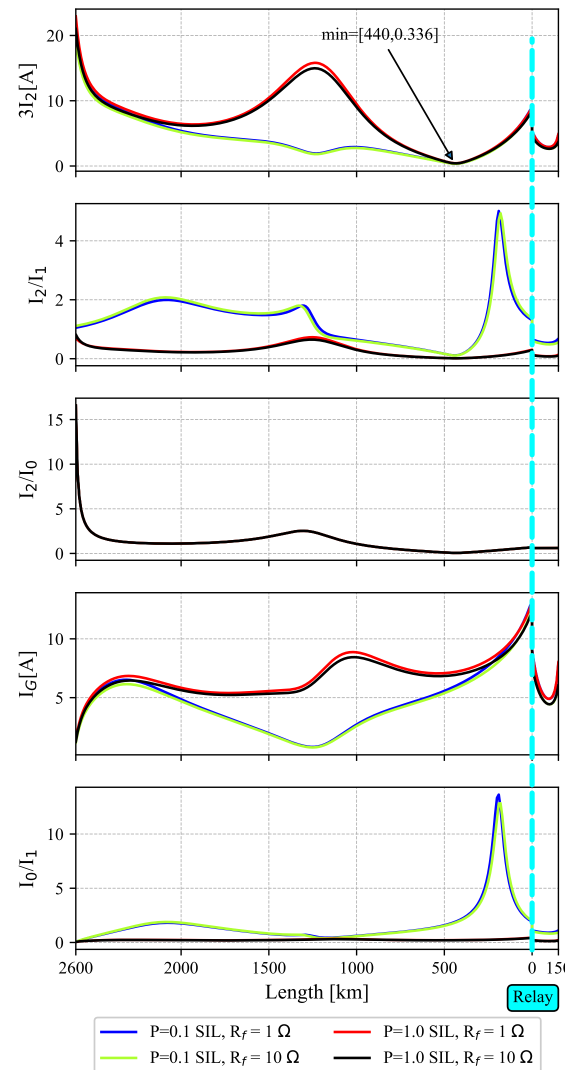

Fig. 5. Curves $3I_2$, I_2/I_1, I_2/I_0, I_G, I_0/I_1 for AG faults

TABLE III
DIRECTIONAL ELEMENT SETTING PARAMETERS FOR SLG FAULTS

Directional Element	Setting Parameters
32QG	50FP=0.25, 50RP=0.25, Z2F=0, Z2R=0.1, a2*=0.02, k2*=0.1
32V	50FP=0.25, 50RP=0.25, Z0F=0, Z0R=0.1, a0=0.04

Note: * – Limited parameter

B. Directional Element Operation

At this stage digital HIL tests were conducted considering the setting obtained with previous two-port element program. The spark-gaps (SG) were modeled as a voltage-controlled switch [19]. The results are summarized in Fig. 6.

It was observed that in AG fault condition the 32QG element did not identify faults in a section of the HWL+ line (denoted by X) because the negative sequence current had low magnitudes in that region (between 400 and 500 km), so the correct parameters setting was compromised. However,

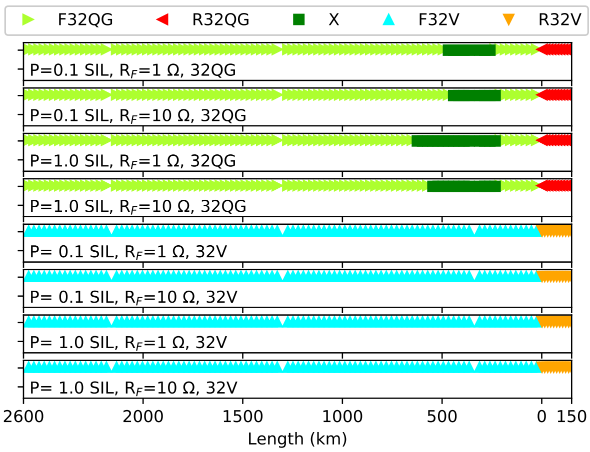

Fig. 6. Directional element performance for AG faults

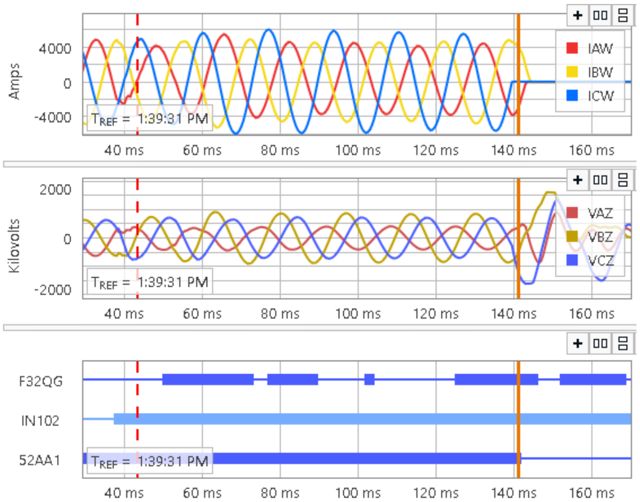

Fig. 7. Oscillography of an AG fault applied to 440 km ahead of the relay (P=1 SIL, R_F= 1 Ω , 32QG)

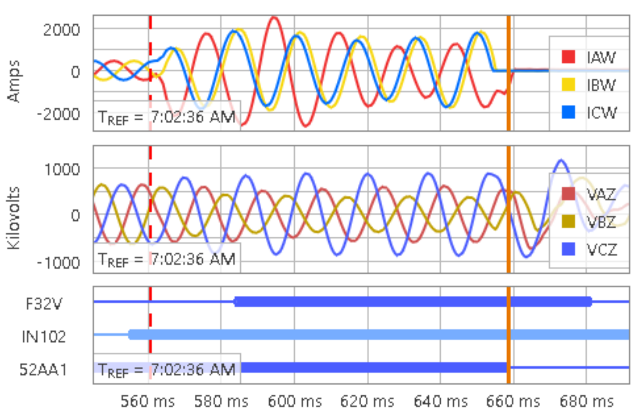

Fig. 8. Oscillography of an AG fault applied to 2349 km ahead of the relay (P=0.1 SIL, R_F= 1 Ω, 32V)

the 32V element properly operated throughout the system. As expected, both elements properly worked for reverse faults.

Voltages and currents measured by the relay and its actuation bits for AG faults are shown in Fig. 7 and Fig. 8. These signals were obtained by two relay events. In Fig. 7, the 32QG element was used. The bit F32QG is activated intermittently during the occurrence of AG fault. The fault application and the circuit-breaker opening are represented by IN102 and 52AA1, respectively. The circuit-breaker opens around 100 ms after the fault occurrence. On the other hand, Fig. 8 shows the performance of the 32V element. In this case, the bit F32V is activated and maintained steady during the entire event.

In addition, it should be mentioned that an incorrect operation means that the bit signal of the directional element is not steady, or the opposite bit is activated. For most of these line sections the bit signal showed a slight distortion.

VII. Conclusions

In the present document it is shown that the two port-network method can be applied to properly calculate relay setting parameters. This phasor calculation is made from the voltage and current measurements at the relay of the system represented by two-port networks.

The study analyzes the performance of regular directional relay element applied for the half-wavelength transmission line (HWL+). HIL tests were implemented with real-time digital simulator (RTDS) and SEL-421 relay. Two-port network element was used to set relay parameters prior to HIL testing.

Some relay parameters could not be set accordingly as they were out of the equipment limits. It was necessary to compromise and use the minimum value for these parameters. However, some parameters should not endanger the relay performance, as regarding the relay global setting. One example is the zero impedance angle of the HWL+ line, which was set to 5°.

Two directional elements were tested (32QG and 32V), obtaining a good performance with the 32V element. It can be said that commercial directional function properly identifies the most frequent transmission line fault, the SLG, at a half-wavelength transmission line.

VIII. Appendix

A. Python program code fragment

```
# HWL+ transmission line parameters

# Sequence Impedances
z0=0.363087342 + 1j*1.28308014  # ohm/km
z1=0.00685620061 + 1j*0.169212229 # ohm/km
z2=0.00685620061 + 1j*0.169212229 # ohm/km


# Sequence Admittances
y0=1j*4.10918334e-06  # mho/km
y1=1j*9.79574755e-06  # mho/km
y2=1j*9.79574755e-06  # mho/km

gamma=np.sqrt(z1*y1) # positive sequence
propagation constant

gamma0=np.sqrt(z0*y0) # zero sequence
```

```
propagation constant

zc1=np.sqrt(z1/y1) # positive sequence
characteristic impedance

zc0=np.sqrt(z0/y0) # zero sequence
characteristic impedance

# 150km transmission line parameters

# Sequence Impedances
z0_2=0.435178486 + 1j*1.44228845 # ohm/km
z1_2=0.016086399 + 1j*0.273432467 # ohm/km
z2_2=0.016086399 + 1j*0.273432467 # ohm/km


# Sequence Admittances
y0_2=1j*3.52372238e-06 # mho/km
y1_2=1j*6.04577024e-06 # mho/km
y2_2=1j*6.04577024e-06 # mho/km


gamma_2=np.sqrt(z1_2*y1_2) # positive
sequence propagation constant

gamma0_2=np.sqrt(z0_2*y0_2) # zero
sequence propagation constant

zc1_2=np.sqrt(z1_2/y1_2) # positive
sequence characteristic impedance

zc0_2=np.sqrt(z0_2/y0_2) # zero
sequence characteristic impedance

# Transmission line two-port network
function
# This represents the matrix of order 6
mentioned in (8) and described by [17]

def Q6x6(g,g_0,l,zc_1,zc_2,zc_0):

    Q_A_120=matrix([[np.cosh(g*l), 0,
    0], [0, np.cosh(g*l), 0],[0, 0,
    np.cosh(g_0*l)]])

    Q_B_120=matrix([[zc_1*np.sinh(g*l),
    0, 0], [0, zc_2*np.sinh(g*l), 0],
    [0, 0, zc_0*np.sinh(g_0*l)]])

    Q_C_120=matrix([[np.sinh(g*l)/zc_1,
    0, 0], [0, np.sinh(g*l)/zc_2, 0],
    [0, 0, np.sinh(g_0*l)/zc_0]])

    Q_D_120=matrix([[np.cosh(g*l), 0,
    0], [0, np.cosh(g*l), 0],[0, 0,
    np.cosh(g_0*l)]])

    Q_6x6=np.concatenate(
    (np.concatenate((Q_A_120,Q_B_120)
    ,1),np.concatenate((Q_C_120,
    Q_D_120),1)))

    return Q_6x6


# HWL+ transmission line two-port network

Q_Z_2600=H6x6_inv*Q6x6(gamma,gamma0,2600,
zc1,zc1,zc0)*H6x6

# 150km transmission line two-port network

Q_Z_150=H6x6_inv*Q6x6(gamma_2,gamma0_2,150,
zc1_2/((500/800)**2),zc1_2/((500/800)**2),
zc0_2/((500/800)**2))*H6x6

Q_A_Z_150_eq=Q_Z_150[0:3,0:3]
Q_B_Z_150_eq=Q_Z_150[0:3,3:6]/4
Q_C_Z_150_eq=Q_Z_150[3:6,0:3]*4
Q_D_Z_150_eq=Q_Z_150[3:6,3:6]

# 150km 4 transmission lines equivalent
two-port network

Q_Z_150_eq=np.concatenate((np.concatenate
((Q_A_Z_150_eq,Q_B_Z_150_eq),1),
np.concatenate((Q_C_Z_150_eq,Q_D_Z_150_eq),
1)))
```

IX. References

[1] M.Tavares, C. Machado, M. Alburqueque, E. Carvalho, M. Araujo, E. Costa, J. Bosco, F. Moreira, R. Fabian, W. de Freitas, C. Faria, A. Peixoto, J. de Lima, and V. Guimares, Power Transmission over long Distances with Half-Wavelength Tecnology. São Paulo, Brazil: Urutau, 2017.

[2] F. Iliceto and E. Cinieri, “Analysis of half-wave length transmission lines with simulation of corona losses,” IEEE Transactions on Power Delivery, vol. 3, no. 4, pp. 2081–2091, 1988.

[3] C. Portela, M. G. Alvim, M. C. Tavares, and M. R. Azevedo, “New conception of long distance transmission lines in alternate current and extra high voltage (in portuguese),” in XX National Seminar on the Production and Transmission of Electric Energy, Recife, Brazil, 2009.

[4] G. Wang, Q. Li, and Zhang, “Research status and prospects of the halfwavelength transmission lines,” in 2010 Asia-Pacific Power and Energy Engineering Conference, Chengdu, China, 2010.

[5] J. S. Ortega and M. C. Tavares, “New perspectives about ac link based on half-wavelength properties for bulk power transmission with flexible distance,” IET Generation, Transmission & Distribution, vol. 12, no. 12, pp. 3005–3012, 2018.

[6] W. D. Stevenson Jr., Elements of Power Systems Analysis. New York, EUA: McGraw-Hill Book Company, 2017.

[7] E. H. Watanabe, A. S. Pedroso, A. C. Ferreira, A. C. S. Lima, R. F. S. Dias, B. Chuco, and S. L. Barcelos, Non-Conventional Alternatives for Electric Power Transmission - Half wave and Segmented CA Transmission (in Portuguese). Brasilia, Brazil: Projeto Transmitir, 2013.

[8] E. C. Gomes, M. C. Tavares, and C. A. Floriano, “Protection scheme for single-phase fault along a half wavelength transmission trunk using conventional relay,” in International Conference on Power Systems Transients, Vancouver, Canada, 2013.

[9] R. G. Fabian and M. C. Tavares, “Using of conventional relays for protecting half-wavelength transmission line from three-phase faults,” in International Conference on Power Systems Transients, Vancouver, Canada, 2013.

[10] F. V. Lopes, B. F. Kusel, K. M. Silva, D. Fernandes, and W. L. A. Neves, "Fault location on transmission lines little longer than half-wavelength," Electric Power Systems Research, vol. 114, pp. 101–109, 2014.

[11] F. Lopes, B. F. Kusel, K. M. Silva, D. Fernandes, and W. L. A. Neves, "Traveling wave-based fault location on half-wavelength transmission lines," IEEE Latin American Transactions, vol. 14, pp. 248–253, 2016.

[12] R. G. F. Espinoza and M. C. Tavares, "Faulted phase selection for half-wavelength power transmission lines," IEEE Transactions on Power Delivery, vol. 33, no. 2, pp. 992–1001, 2018.

[13] K. Zimmerman and D. Costello, "Fundamentals and improvements for directional relays," in 63rd Annual Conference for Protective Relay Engineers, Texas, EUA, 2010.

[14] G. Kindermann, Power System Protection (in Portuguese). Florianopolis, Brazil: Geraldo Kindermann, 2005.

[15] S. E. Laboratories, SEL-421 Relay Protection and Automation System Instruction Manual. SEL Inc., 2011.

[16] S. Ghosh, Network Theory: Analysis and Synthesis. New Delhi, India: Phi Learning, 2009.

[17] M. E. Z. Alcahuaman, "Sensitivity analysis of secondary arc current for different transmission lines (in portuguese)," M. Eng. thesis, School of Electrical and Computer Engineering (UNICAMP), São Paulo, Brazil, 2007.

[18] J. S. A. Sarmiento and M. C. Tavares, "Methodology for optimizing the capacity and costs of overhead transmission lines by modifying their bundle geometry," Electric Power Systems Research, vol. 163, pp. 668–677, 2018.

[19] J. A. S. Ortega and M. C. Tavares, "Analysis of half-wavelength transmission line under critical balanced faults: Voltage response and overvoltage mitigation procedure," Electric Power Systems Research, vol. 166, pp. 99–111, 2019.

[20] R. F. Vidigal, "Analysis of the behavior of an isolated transmission line with a little more than half wave length for different operating conditions in steady state and during the energization manouver (in portuguese)," M. Eng. thesis, School of Electrical and Computer Engineering (UNICAMP), São Paulo, Brazil, 2010.

[21] O. F. R. Dias and M. C. Tavares, "Implementation and performance evaluation of a harmonic filter for use in adaptive single-phase reclosing," IET Generation, Transmission & Distribution, vol. 11, no. 9, pp. 2261–2268, 2017.

[22] W. A. Elmore, Protective Relaying Theory and Applications. New York, EUA: Marcel Dekker, Inc., 2003.

[23] J. G. Andrichak and S. C. Patel, "Polarizing sources for directional ground relays," General Electric, Tech. Rep. GER-3182A, 1998.